International Journal of Advanced Multidisciplinary Research and Studies

The Mean-square Relative Displacement of Iron in Anharmonic XAFS Theory

[1] Nguyen Thi Minh Thuy, [2] Le Quang Thanh
[1, 2] Faculty of Fundamental Sciences, University of Fire Prevention & Fighting, Hanoi 120602, Vietnam

　　　　Corresponding Author: **Le Quang Thanh**

Abstract

Mean-square relative displacement (MSRD) of Iron (Fe) has been investigated in the anharmonic X-ray absorption fine structure (XAFS) theory. The thermodynamic parameters are derived from the influence of the absorbing and backscattering atoms of all their nearest neighbors in the crystal lattice with thermal vibrations. The MSRD is calculated in explicit forms using the classical anharmonic correlated Einstein model. The numerical results of Fe in the temperature range from 0 to 600 K are in good agreement with those obtained by the other theoretical models and an experiment at several temperatures. The analytical results show that the present model is useful in analyzing the experimental XAFS data of Fe.

Keywords: XAFS Debye-Waller factor, Crystalline Iron, Einstein Model, Classical Statistical Theory

1. Introduction

Nowadays, X-ray absorption fine structure (XAFS) spectroscopy can contain information on local structures around X-ray absorbing atoms and gives interatomic distances and coordination numbers in crystal lattices [1]. The K-edge XAFS signal includes a non-Gaussian disorder for a given scattering path is expressed in terms of a canonical average of all distance-dependent factors by [2].

$$\chi(k,T) = \frac{N e^{-2k^2\sigma^2(T)} f(k)}{k R^2(T)} \sin\left[2kR(T) + \delta(k)\right]$$

(1)

Where k is the wave number of the photoelectron, $f(k)$ and $\delta(k)$ characterizes scattering parameters of the photoelectron, $\sigma^2(T)$ is the mean-square relative displacement (MSRD) describes the thermal disorder in the neighbor distance, $R(T)$ is the distance to the neighboring atom, and N is the number of neighboring atoms.

Currently, the temperature-dependent XAFS parameters are a topical issue that receives the attention of many scientists around the world [3]. It is because the XAFS signal will smear out under the effect of thermal disorders that cause anharmony [4]. In the anharmonic XAFS signal analysis, the mean-square relative displacement (MSRD) $\sigma^2(T)$ is an important thermodynamic parameter because it can characterize the anharmonic XAFS properties [5]. In recent years, crystalline iron (Fe) has accounted for over 90% of worldwide metal production [6], which is the most widely used of all metals because it is often used to create steel in civil engineering and manufacturing [7]. Meanwhile, the experimental values at 293 K, 313 K, 333 K, 353 K, 373 K, and 393 K were measured MSRD of Fe at the Synchrotron Radiation Siberian Center (SRSC), Russia, by Pirog *et al.* [8].

Recently, a classical anharmonic correlated Einstein (CACE) model has been applied to effectively treat the anharmonic XAFS parameters of metals [9]. This model has the advantage that the expressions of the anharmonic XAFS parameters are obtained in explicit and simple forms, so it is very convenient to analyze anharmonic XAFS data in the range of temperatures not too low [10]. Still, it has not yet been used to analyze the anharmonic XAFS parameters of Fe. Hence, investigating the MSRD of Fe based on the CACE model will be a necessary addition to the experimental XAFS analysis technique.

2. Formalism and calculation model

In the anharmonic XAFS theory, the MSRD can describe the anharmonic XAFS amplitude reduction [11]. This thermodynamic parameter is explicitly related to low-order moments of true RD function, which can be determined as follows [12]:

$$MSRD = \left\langle (r - \langle r \rangle)^2 \right\rangle = \left\langle (x - \langle x \rangle)^2 \right\rangle = \left\langle x^2 \right\rangle - \left\langle x \right\rangle^2 \tag{2}$$

Where the angular bracket $\langle \ \rangle$ is the thermal average, x is the deviation distance between the backscattering and absorbing atoms, and r is the instantaneous bond length between atoms.

To determine the thermodynamic parameters of a system, it is necessary to specify its anharmonic effective (AE) potential and force constants [13]. The AE potential in the relative vibrations of backscattering (A) and absorbing (B) atoms can be calculated from the pair interaction (PI) potential [14]:

$$V_{eff} = \varphi(x) + \sum_{i=A,B} \sum_{j \neq A,B} \varphi\left(\varepsilon_i x \hat{R}_{AB} \hat{R}_{ij} \right), \ \ \varepsilon_i = \frac{\mu}{M_i}, \tag{3}$$

Where $\mu = M_A M_B / (M_A + M_B)$ is the reduced mass of the backscatter with masse M_A and absorber with masse M_B, sum i is the over backscatter ($i = A$) and absorber ($i = B$), the sum j is over the nearest neighbors, $\hat{R}$ is a unit vector, $\varphi(x)$ is a PI potential of these atoms, $\varphi\left(\varepsilon_i x \hat{R}_{AB} \hat{R}_{ij} \right)$ express the contribution of nearest-neighbor atoms to $\varphi(x)$.
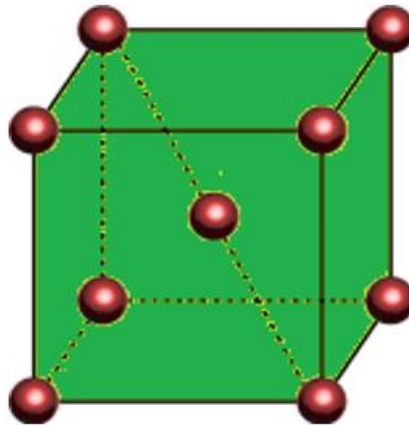

Fig 1: The structural model of Fe.

The structural model of Fe is illustrated in Fig 1, which is a body-centered cubic (BCC) arrangement. This structure has similar atoms at one center and eight corners of a cube [15], so each atom has a mass of m, and each unit cell contains two atoms [16]. After using structural characteristics, the AE potential of Fe is calculated from Eq. (3) and is written as

$$V_{eff}(x) = \varphi(x) + \varphi(0) + 2\varphi\left(-\frac{1}{2}x \right) + 6\varphi\left(-\frac{1}{6}x \right) + 6\varphi\left(\frac{1}{6}x \right), \tag{4}$$

Usually, the Morse potential can validly determine the PI potential of the crystals [17]. If this potential is expanded up to the three orders around its minimum position, it can be written as

$$\varphi(x) = D\left(e^{-2\alpha x} - 2e^{-\alpha x} \right) \cong -D + D\alpha^2 x^2 - D\alpha^3 x^3 + \frac{7}{12} D\alpha^4 x^4, \ x = r - r_0, \tag{5}$$

Where D is the dissociation energy, α is the width of the potential, and r_0 is the equilibrium bond length between atoms.

The result of AE potential can be obtained from Eq. (4) using Morse potential in Eq. (5). If ignoring the overall constant, it is presented in the form:

$$V_{eff}(x) = \frac{1}{2} k_{eff} x^2 - k_{an3} x^3 + k_{an4} x^4, \tag{6}$$

Where k_{eff} is the effective force constant, and k_{an3} and k_{an4} are anharmonic force constants, which are not the temperature-dependent and are written as

$$k_{eff} = \frac{11}{3} D\alpha^2, \ \ k_{an3} = \frac{3}{4} D\alpha^3, \ \ k_{an4} = \frac{1715}{2592} D\alpha^4, \tag{7}$$

The CACE model [9] is derived from the correlated Einstein model [18] using the AE potential [14] and classical statistical theory [19]. In this model, each atomic thermal vibration in the crystal lattice can be treated as a phonon and characterized via the correlated Einstein temperature θ_E and frequency ω_D [10]. These parameters of Fe can be defined from the effective force

constant as follows:

$$\omega_E = \sqrt{\frac{k_{eff}}{\mu}} = \alpha \sqrt{\frac{22D}{3m}}, \quad \theta_E = \frac{\hbar \omega_E}{k_B} = \frac{\hbar \alpha}{k_B} \sqrt{\frac{22D}{3m}},$$

(8)

Where $\hbar$ is the reduced Planck constant and k_B is the Boltzmann constant.

In the classical-statistical limit, the moments $\langle x^k \rangle$ can be determined by evaluating the thermal average in the third-order approximation [19]:

$$\langle x^k \rangle = \frac{\int_{-\infty}^{\infty} x^k \exp\left[-\frac{V_{eff}(x)}{k_B T}\right] dx}{\int_{-\infty}^{\infty} \exp\left[-\frac{V_{eff}(x)}{k_B T}\right] dx} \approx \frac{\int_{-\infty}^{\infty} x^k \exp\left[\frac{-k_0 x^2}{2k_B T}\right] \left[\sum_{n=0}^{3} \frac{1}{n!} \left(\frac{k_3 x^3 - k_4 x^4}{k_B T}\right)^k\right] dx}{\left(\frac{2\pi k_B T}{k_0}\right)^{1/2} \left[1 + \frac{3(k_B T)}{k_0^2}\left(\frac{5k_3^2}{2k_0} - k_4\right)\right]}$$

(9)

The temperature-dependent general expressions of the MSRD in the CACE model were calculated using Eqs. (2) and (9) by Stern *et al.* [19]. Substituting the expressions of local force constants k_{eff}, k_{an3}, and k_{an4} of Fe in Eq. (7) into this expression of the MSRD, we obtain the following result:

$$MSRD(T) \Box \frac{k_B T}{5D\alpha^2}\left(1 + \frac{47k_B T}{400D}\right) \approx \frac{k_B T}{5D\alpha^2},$$

(10)

Thus, the CACE model has been extended to efficiently calculate the temperature-dependent. MSRD of Fe in the anharmonic XAFS theory. The obtained expressions using this model can satisfy all their fundamental properties in the temperature-dependent.

3. Results and discussion
In this section, the numerical results of Fe are calculated using the Matlab software [20] based on the obtained expressions in Secs. 2 and their physical parameters. The values of Morse potential parameters D and α, atomic mass m, correlated Einstein temperature θ_E and frequency ω_E, and local force constants k_{eff}, k_{an3}, and k_{an4} of Fe are given in Table 1.

Table 1: The physical parameters of Fe and its thermodynamic parameters are obtained using the CACE and experiment

Method	m (u)	D (eV)	α (Å^{-1})	k_{eff} (eVÅ^{-2})	k_{an3} (eVÅ^{-3})	k_{an4} (eVÅ^{-4})	ω_E ($\times 10^{13}$Hz)	θ_E (K)
This work	55.845	0.4174	1.3885	2.9506	0.8380	1.0265	3.1836	243.2
Experiment [8]		0.42±0.12	1.40±0.2	4.0±0.5	1.7±0.7	2.0±2.0	3.3186±0.2880	253.5±21.9

Our obtained results using the CACE model are calculated from Eqs. (7)-(8). And the experimental values measured at the SRSC, Russia, by Pirog & Nedoseikina [8], in which the correlated Einstein temperature and frequency are derived from the effective force constant. It can be seen that our results agree with the experimental values, especially for the correlated Debye temperature and frequency.
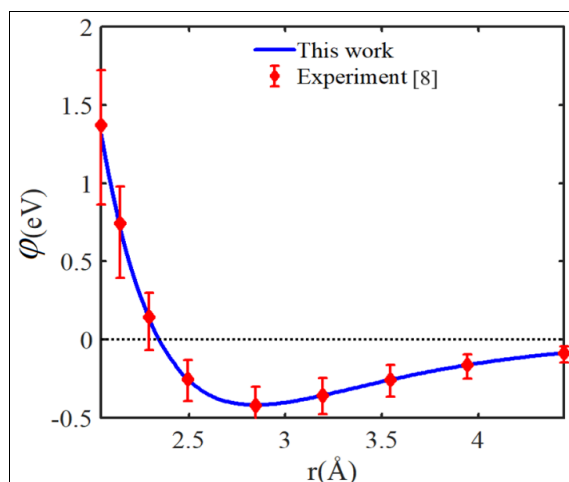

Fig 2: The distance-dependent Morse potential of Fe is obtained from the CACE model and experiment.

The distance dependence of the Morse potential $V(r-r_0)$ of Fe is calculated using Eq. (5), with the Morse potential parameters given in Table 1, which is shown in Fig 2. It can be seen that our result agrees better with those obtained from the experimental data [8], especially in the vicinity of equilibrium bond lengths.
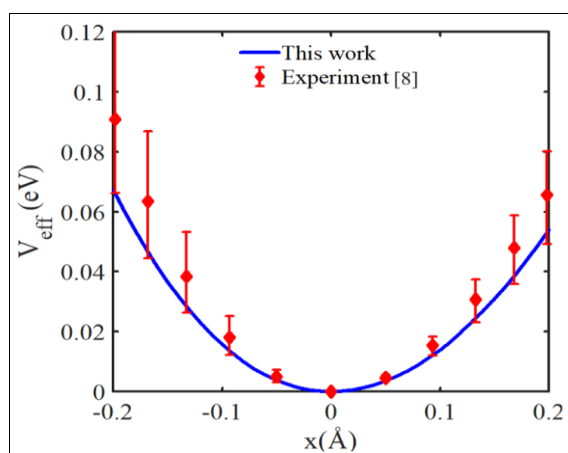
Fig 3: The position-dependent AE potential of Fe is obtained from the CACE model and experiment

The position dependence of the AE potential $V_{eff}(x)$ of Fe is calculated using Eqs. (6)-(7) with the local force constants are given in Table 1, which is shown in Fig 3. It can be seen that our result agrees better with those obtained from the experimental data [8], especially near the equilibrium position (x = 0). In addition, our obtained result using the CACE model is similar to those obtained with the quantum-correlated Einstein (QACE) [21] and correlated Debye (ACD) [22] models because all three models use the AE potential [14].
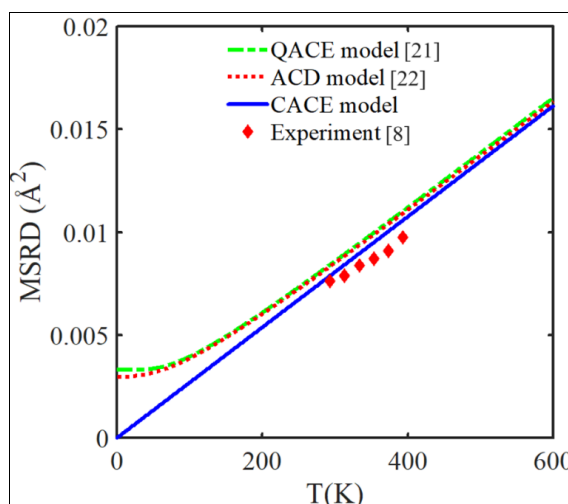
Fig 4: Temperature-dependent MSRD of Fe is obtained using the CACE, QACE, and ACD models and experiment

The temperature dependence of the $MSRD(T)$ of Fe in a range from 0 to 600 K is illustrated in Fig 4. Our obtained result using the CACE model is calculated by Eq. (10). It can be seen that our results are in agreement with those obtained using the QACE [21] and ACD [22] models and experiment [8]. For example, the obtained results using the CACE model, QACE model, ACD model, and experiment at $T \approx 293$ K are $\sigma^2 \Box 7.9 \times 10^{-3}$ Å^2, $\sigma^2 \Box 8.4 \times 10^{-3}$ Å^2 [21], $\sigma^2 \Box 8.3 \times 10^{-3}$ Å^2 [22], and $\sigma^2 \Box 7.6 \times 10^{-3}$ Å^2 [8], respectively. Moreover, our obtained result reaches zero as the temperature reaches zero, so the CACE model is unsuitable in the low-temperature region because this model only uses classical statistical theory [19] in calculations. However, the CACE model still works effectively at temperatures that are not too low (T > θ_E), so our obtained result can be used well at room temperature, as seen in Fig 4.

4. Conclusion

In this work, we have expanded a calculation model to effectively analyze the MSRD of Fe in the anharmonic XAFS theory. The calculated expressions using the present CACE model satisfied all of their fundamental properties in the temperature-dependent. The MSRD increases linearly with increasing temperature *T* because the anharmonic XAFS amplitude increases more intensely at higher temperatures. This thermodynamic property shows that the higher the temperature, the stronger the X-ray absorption of Fe. These results can also describe the influence of anharmonic effects on the XAFS signal at temperatures above the correlated Einstein temperature θ_E. Our numerical results of Fe agree with those obtained using the QACE and

ACD models and an experiment at various temperatures. This agreement shows the effectiveness of the present model in investigating the MSRD of Fe in the anharmonic XAFS theory.

5. Acknowledgments

6. References

1. Yokoyama T, Kobayashi K, Ohta T, Ugawa A. Anharmonic interatomic potentials of diatomic and linear triatomic molecules studied by extended x-ray-absorption fine structure, Physical Review B. 1996; 53:6111-6122.
2. Newville M. Fundamentals of XAFS, Reviews in Mineralogy & Geochemistry. 2014; 78(1):33-74.
3. Fornasini P, Grisenti R. On EXAFS Debye-Waller factor and recent advances. Journal of Synchrotron Radiation. 2015; 22:1242-1257.
4. Eisenberger P, Brown GS. The study of disordered systems by EXAFS: Limitations, Solid State Communications. 1979; 29(6):481-484.
5. Greegor RB, Lytle FW. Extended x-ray absorption fine structure determination of thermal disorder in Cu: Comparison of theory and experiment, Physical Review B. 1979; 20(12):4902-4907.
6. Emsley J. (eds), Nature's Building Blocks: An A-Z Guide to the Elements, 2nd edition, Oxford University Press, Oxford, 2011.
7. Smith WF, Hashemi J. (eds), Foundations of Materials Science and Engineering, 4th edition, McGraw-Hill Book, New York, 2006.
8. Pirog IV, Nedoseikina TI. Study of effective pair potentials in cubic metals, Physica B. 2003; 334:123-129.
9. Tien TS, Hung NV, Tuan NT, Nam NV, An NQ, Thuy NTM, *et al*. High-order EXAFS cumulants of diamond crystals based on a classical anharmonic correlated Einstein model. Journal of Physics and Chemistry of Solids. 2019; 134:307-312.
10. Tien TS. Temperature-Dependent EXAFS Debye-Waller Factor of Distorted HCP Crystals. Journal of the Physical Society of Japan. 2022; 91:054703.
11. Tröger L, Yokoyama T, Arvanitis D, Lederer T, Tischer M, Baberschke K. Determination of bond lengths, atomic mean-square relative displacements, and local thermal expansion by means of soft-x-ray photoabsorption, Physical Review B. 1994; 49(2):888-903.
12. Fujikawa T, Miyanaga T. Quantum Statistical Approach to Debye-Waller Factors in EXAFS, EELS and ARXPS. I. Anharmonic Contribution in Plane-Wave Approximation, Journal of the Physical Society of Japan. 1993; 62(11):4108-4122.
13. Yokoyama T, Kobayashi K, Ohta T, Ugawa A. Anharmonic interatomic potentials of diatomic and linear triatomic molecules studied by extended x-ray-absorption fine structure, Physical Review B. 1996; 53(10):6111-6122.
14. Hung NV, Rehr JJ. Anharmonic Correlated Einstein-Model Debye-Waller Factors, Physical Review B. 1997; 56(1):43-46.
15. Simon SH. The Oxford Solid State Basics, 1st edition, Oxford University Press, Oxford, 2013.
16. Shabalin IL. Ultra-High Temperature Materials I, Springer, New York, 2014.
17. Girifalco LA, Weizer VG. Application of the Morse Potential Function to Cubic Metals, Physical Review. 1959; 114(3):687-690.
18. Sevillano E, Meuth H, Rehr JJ. Extended x-ray absorption fine structure Debye-Wailer factors. I. Monatomic crystals. Physical Review B. 1979; 20(12):4908-4911.
19. Stern EA, Livins P, Zhang Z. Thermal vibration and melting from a local perspective. Physical Review B. 1991; 43(11):8850-8860.
20. Peng L, Bao L, Huang M. Application of Matlab/Simulink Software in Physics. In: Y. Wu (eds), High Performance Networking, Computing, and Communication Systems, ICHCC 2011, Communications in Computer and Information Science 163, Springer, Berlin, 2011.
21. Tien TS. Extending quantum anharmonic correlated Einstein model in studies of anharmonic EXAFS Debye-Waller factor of BCC structure metals. European Physical Journal Plus. 2022; 137:1009.
22. Hung NV, Hue TT, Khoa HD, Vuong DQ. Anharmonic correlated Debye model high-order expanded interatomic effective potential and Debye-Waller factors of bcc crystals, Physica B. 2016; 503:174-178.